2010

Observation of a Characteristic Length Scale in the Healing of Glassy Polymer Interfaces

Guangcui Yuan
Clive Li
Sushil K. Satija
Alamgir Karim, *University of Akron*
Jack F. Douglas, *University of Akron Main Campus*, et al.

Observation of a characteristic length scale in the healing of glassy polymer interfaces†

Guangcui Yuan,[ab] Clive Li,[b] Sushil K. Satija,[b] Alamgir Karim,‡[*c] Jack F. Douglas[*c] and Charles C. Han[a]

We examine the evolution ('healing') of the interface between two polymer films at various temperatures below the glass transition temperature, T_g. Specifically, neutron reflectometry is used to study the relaxation of the interface between both unentangled and entangled deuterated polystyrene (d-PS) and hydrogenated polystyrene (h-PS) films in the glass state where these bilayer films are supported on silicon substrates. We find that the initially sharp interface between the glassy polymer layers broadens with time (t), but the average interfacial thickness $\Delta\sigma(t)$ between these layers then saturates after long time to a thickness (ξ_p) in a range between 1 nm and 3 nm after a long annealing time ($\gtrsim 1$ h) for the range of temperatures investigated. This characteristic scale, and the temperature dependence of the interfacial relaxation time τ, were unanticipated, and we thus investigated the dependence of ξ_p and τ on molecular mass (M), annealing temperature (T) and the thickness (h_f) of the PS films. We find that ξ_p increases with h_f at a fixed T and increases with T at fixed h_f. Our observation of a 'healing length' ξ_p, regardless of whether the polymers are entangled or not, and the dependence of ξ_p on T rule out an interpretation of this parameter in terms of the reptation model. On the other hand, ξ_p has a scale comparable to the mobile interfacial layer thickness reported in both small molecule and polymeric materials in the glass state, suggesting that ξ_p is a well-defined dynamical length scale characterizing the interfacial properties of glassy materials. The existence of such an interfacial layer has numerous implications for the processing and scientific understanding of thin polymer films.

Introduction

Many advanced technologies, such as nanoimprinting and advanced lithographic fabrication, as well as materials development areas such as gas separation membranes, solar cell development, etc., rely on the unique properties of high molecular mass polymer films. Taking full advantage of the functional properties of these films in the design of these new materials requires improved metrologies that enable the control of film properties. In the present work, we address a central issue of broad technological and scientific interest—how do chain entanglement and glass formation alter the evolution of polymer interfaces brought into contact? The observations of the present study are contrasted with prior observations on interdiffusion between polymer films that have been made at more elevated temperatures than our glass state measurements.

There have been numerous previous observations of the intermixing of two polymer films brought in contact and annealed above T_g. The short time dynamics of this process has been examined by neutron reflectometry,[1–10] which quantifies the interdiffusion process at sub-nanometre resolution when the interfacial widths (σ) are between 0.5 nm to 20 nm.[11,12] An examination of these former polymer thin film inter-diffusion measurements indicates some general trends:[13] (1) annealing above T_g leads to a relatively rapid initial interfacial broadening over a scale of approximately 2 nm which is sometimes called the 'burst effect';[14,15] (2) at intermediate annealing times, no significant interfacial broadening occurs; (3) next, there is a long time regime where the interface width increases with time t according to an approximately power law scaling, $\sigma \approx t^{1/4}$; (4) finally, at very long t, normal Fickian diffusion is found, corresponding to a power law interfacial broadening in t, $\sigma \approx t^{1/2}$. This long time diffusive interfacial broadening has been measured by a variety of techniques such as forward-recoil spectrometry[16] and secondary-ion mass spectrometry.[17,18] The relatively rapid evolution in the interfacial width on a scale of ≈ 2 nm takes place during the initial heating of the sample at short times. This fast relaxation process has been interpreted theoretically as a reptative chain motion within a tubular region defined by surrounding polymer chain segments.[19–21] Unfortunately, this high frequency relaxation process is much too rapid to be accommodated by this molecular model. Molecular-dynamics simulation[22] and spin-echo experiments[23] in bulk polymers also fail to confirm the confined reptation model predictions for this fast interfacial

[a]State Key Laboratory of Polymer Physics and Chemistry, Joint Laboratory of Polymer Science and Materials, Institute of Chemistry, Chinese Academy of Sciences, Beijing, 100190, People's Republic of China
[b]Center for Neutron Research, National Institute of Standards and Technology, Gaithersburg, Maryland, 20899, USA
[c]Polymers Division, National Institute of Standards and Technology, Gaithersburg, Maryland, 20899, USA. E-mail: jack.douglas@nist.gov; Tel: +1 301 975 6779; alamgir@uakron.edu; +1 330 972 7500
† Contribution of the National Institute of Standards and Technology—Work not subject to copyright in the United States.
‡ Present address: College of Polymer Science and Polymer Engineering, University of Akron, Akron, OH, 44325-3909, USA.

broadening. This deviation between theory and experiment was then attributed to the uncertainty in the initial conditions describing the polymer chains at the interface.[13,24] At present, there is no generally accepted molecular model of this interfacial relaxation phenomenon. Experimentally, it is not even clear that entanglement is relevant to this phenomenon, and we consider this issue below simply by examining whether this effect exists in unentangled polymer films.

The distorted nature of the chain conformation at the interface relative to the bulk, the possible non-uniform distribution of chain ends, interfacial fluctuations due to capillary waves, and the influence of polymer–substrates interaction are all factors that could possibly contribute to the fast interfacial relaxation, but these effects are difficult to quantify theoretically and experimentally.[14,15,25–27] Substantial efforts have been made to address these expected conformational changes, both from experimental and theoretical standpoints. For example, Kuhlmann et al.[8] have investigated the effects of the confined geometry and substrate interaction on the initial stages of interdiffusion in polystyrene films and found the interfacial broadening to be extremely limited in thin glassy films. Lin et al.[28,29] measured the reduced mobility of poly(methyl methacrylate) films near the native oxide surface of silicon as a function of distance from the surface and found that the effective range of the substrate on the interdiffusion dynamics was a scale in a range between 30 nm and 40 nm. Details of the initial stages of the layer interdiffusion process are not well understood and further experiments are evidently necessary.

Since this interfacial diffusion process is difficult to resolve at temperatures above T_g due to relatively high molecular mobility, we decided to approach the problem by annealing the sample for long times *below* T_g. This procedure allowed us to focus instead on the initial stage of interfacial relaxation between polymer interfaces, which is particularly poorly understood. Specifically, we examine the interfacial evolution of a d-PS/h-PS bilayer by annealing at temperatures (85 °C to 95 °C) below the bulk T_g of polystyrene ($T_g \approx 103$ °C). Molecular mass and film thickness effects were also investigated since they inform about the physical nature of the interface broadening process. In particular, we varied the molecular mass from below to above the critical molecular mass of PS (38 K molecular mass)[30] to gain some insight into the role of chain entanglement on interfacial broadening in the glass state.

Experimental

Sample preparation

A series of PS bilayer samples was prepared on polished silicon substrates (7.5 cm diameter, 0.5 cm thickness). Each bilayer sample had a nearly matching relative molecular mass M between the d-PS (Polymer Source Inc.) and the h-PS (Aldrich Chem. Com.): 33 000/32 660, 115 000/114 200, and 673 600/641 340 (unit is g mol^{-1}) with R_g values of 4.8 nm, 9.0 nm, 21.4 nm, respectively. Each polymer has a polydispersity $k \equiv M_w/M_n$ less than 1.1 (M_w and M_n denote mass (weight) averaged and number averaged molecular mass).[31] The d-PS/h-PS bilayer samples were prepared by spin-coating and floating technique. The first layer of d-PS was spun-cast onto the

hydrophilic surface of one Si wafer. By immersing the wafer into distilled water, the d-PS layer was floated off onto the water surface and was then picked up on another Si wafer spin-coated with h-PS prepared in advance. X-Ray reflectometry was used to characterize the single films and bilayer films with respect to film thickness and surface roughness. An ultraviolet (UV)/ozone cleaner was used to clean the silicon wafers, and an oxide layer was formed on the polished silicon substrates. The thickness of the oxide layers was measured by X-ray reflectometry[32,33] to be in a range between 1.0 nm and 1.5 nm and the root mean square value thickness of this layer was determined to be in a range between 0.1 nm to 0.5 nm. Residual solvent can be a problem in cast polymer films so the bilayer films were placed under vacuum at 60 °C for about 12 h to remove residual solvent and water trapped between the layers before used. Samples were subsequently annealed for different times at desired temperatures and quenched to room temperature for the neutron measurements.

Neutron reflectometry

The neutron reflectivity measurements were performed at the National Institute of Standards and Technology Center for Neutron Research (NCNR) advanced neutron diffractometer/ reflectometer (AND/R) or NG-7 reflectometry. The description and characteristics of AND/R and NG-7 reflectometry are given elsewhere.[34,35] The wavelength (λ) of the neutron used is 0.4993 nm at the AND/R and 0.4768 nm at NG-7 reflectometry instruments with $\Delta\lambda/\lambda$ both around 0.025. The reflectivity measurements were performed over a range of angles and we present our data as a function of the neutron momentum transfer perpendicular to the surface, $q = (4\pi/\lambda)\sin \theta$, where θ is the incident angle of the neutron radiation. The angular divergence of the beam was varied through the reflectivity scan and this provided a relative q resolution $\Delta q/q$ of 0.04. Since reflectivity observations are sensitive to the neutron scattering length density profile perpendicular to the sample surface, the elastic coherent-scattering per unit volume q_c^2 was used to determine the concentration profiles. q_c^2 is defined in terms of the neutron scattering length, b, through the relation, $q_c^2 = 16\pi n b$, where n is the number density of the scattering nuclei. q_c^2 values for d-PS, h-PS, silicon oxide and bulk silicon are 3.21×10^{-2}, 7.03×10^{-3}, 1.71×10^{-2} and 1.04×10^{-2} nm^{-2}, respectively. Programs from the Reflpak Suite were utilized for our data reduction and analysis.[36]

Results and discussion

A typical set of neutron reflectivity profiles is shown in Fig. 1a and b. We analyze the NR data using a two-layer model, representing two thin homopolymer films, on a very thin native Si oxide layer.[32,33] Solid lines denote the fitted reflectivity curves where the corresponding scattering length density profiles are shown in the inset. The best-fit profiles were determined by a minimization of the least-squares deviation of the data to the model. The range of uncertainty in each fitted parameter was determined by fixing that parameter at various values and allowing the other parameters to vary in the fitting within physically reasonable limits and in this way the maximum uncertainty of the fitted parameters in comparison to the data
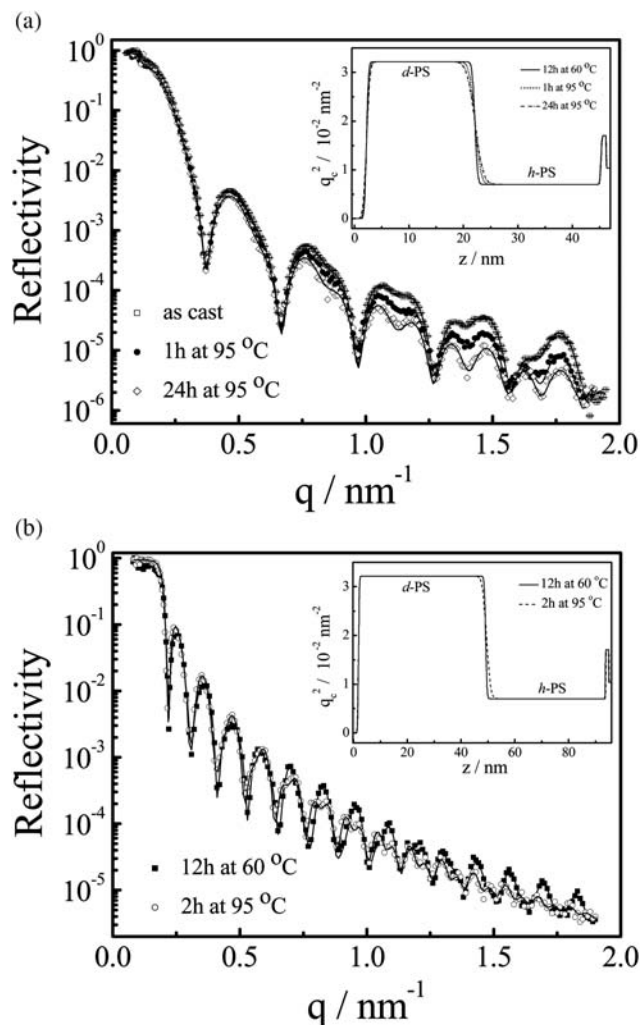
Fig. 1 Typical neutron reflectivity data from bilayer samples. The data are shown with the symbols and the best fits are given by the solid lines. Real space profiles in terms of q_c^2 corresponding to the best-fit curves for the neutron reflectivity data are shown as inset in the respective figure. (a) d-PS(115 000 g mol^{-1}, 20.0 nn)/h-PS(114 200 g mol^{-1}, 23.1 nm); (b) d-PS(115 000 g mol^{-1}, 46.9 nm)/h-PS(114 200 g mol^{-1}, 44.4 nm).

was found to be about 5%. The data of Fig. 1a correspond to a bilayer of d-PS (115 000 g mol^{-1}, 20.0 nm) placed above a h-PS (114 200 g mol^{-1}, 23.1 nm) film and the measurements were taken after annealing the bilayer at 95 °C for 1 h and 24 h, respectively. The data in Fig. 1b correspond to a bilayer comprised of an upper layer of d-PS (115 000 g mol^{-1}, 46.9 nm thick) on a layer of h-PS (114 200 g mol^{-1}, 44.4 nm thick) where the bilayer film was annealed at 95 °C for 2 h. The initial thickness h_f of the deuterated layer is determined by the q spacing between the minima or maxima of the reflectivity curve, these characteristic distances scaling inversely with the q values at which these intensity extrema occur. Several distinct interface fringes in the reflectivity curve are observed, indicating that the interfaces are relatively sharp. The modulation periods do not shift after annealing so that the thermal treatment does not change the layer thickness. When the interface between the layers begins to broaden, it results in a gradual loss of higher order minima in the reflectivity curves at high q values.

Assuming that the interfacial roughness of the interfaces is Gaussian distributed and that a close contact exists between the layers (as it typically found for floated bilayer films), the refractive index profiles at the interfaces can be described by error functions with a characteristic parameter σ. We assume that σ has contributions from the initial film roughness, σ_0, and the interfacial broadening arising during thermal annealing so that these contributions are separated in our analysis. We then corrected σ by assuming that the initial roughness and subsequent inter-diffusion are independent and that σ_0 is constant during the annealing experiment, *i.e.*, $\Delta\sigma = \sqrt{\sigma_t^2 - \sigma_0^2}$. $\Delta\sigma$ can be taken as a measure of the interfacial broadening in the bilayer and in Fig. 2 we show $\Delta\sigma$ as a function of t at three annealing temperatures, where the samples have essentially the same thickness (see Table 1). It can be seen that $\Delta\sigma(t)$ increases with annealing time for about 6 h and then $\Delta\sigma(t)$ becomes nearly constant. We describe this kinetics by a first order rate process with a power law rate,[37,38]

$$\Delta\sigma = \xi_p\{1 - \exp[-(t/\tau)^\alpha]\},\qquad(1)$$

where $\xi_p = \Delta\sigma(t \to \infty)$ describes the long time 'plateau value' of $\Delta\sigma$, τ denotes the characteristic evolution time and α is an exponent governing the time dependent growth rate. This simple model provides a good description of our data. The solid lines, which represent best-fits to the experimental data, are shown in Fig. 2–4 and χ^2 values are given in Table 1. The trend shown for all these figures is similar for all our bilayer films and Table 1 summarizes the parameters (ξ_p, τ, α) on which our discussion below revolves.

An examination of $\Delta\sigma(t)$ in Fig. 2–4 indicates a common pattern consistent with eqn (1). First, there is a rapid evolution of $\Delta\sigma(t)$ on a timescale on the order of 1 h, where this timescale is not particularly sensitive on T, M and h_f. After this relaxation time τ (see Table 1) on the order $O(1$ h), the mean interfacial width $\Delta\sigma(t)$ exhibits a plateau that we define as ξ_p. The time dependence of the interfacial relaxation is well-described by a stretched exponential function [eqn(1)], as typical for relaxation in glass-forming liquids.[39] In some cases, the data are too
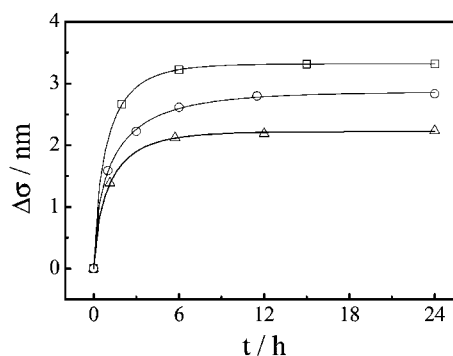

Fig. 2 Interfacial broadening, $\Delta\sigma$, plotted as a function of time (t), for samples (a–c) prepared with the same pair of polymer d-PS(115 000 g mol^{-1})/h-PS(114 200 g mol^{-1}) and with thickness h_f of each layer about 45 nm, but annealed at 95 °C (sample a: □), 90 °C (sample b: ○) and 85 °C (sample c: △), respectively. The solid lines correspond to best-fit to eqn (1). See Table 1 for χ^2 values for fits.
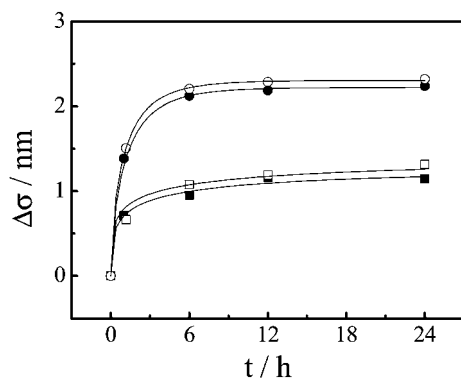
Fig. 3 Interfacial broadening, $\Delta\sigma$, plotted as a function of time (t), for samples (c–f) annealed at 85 °C. For sample d (■) and sample e (□), the thickness h_f of each layer is about 20 nm, which is about $2R_g$ for chains with molecular mass of 110 K (sample d) and $1R_g$ for chains with $M = 670$ K (sample e). For sample c (●) and sample f (○), the thickness h_f of each layer is about 45 nm, which is about $5R_g$ for chains with molecular mass of 110 K (sample c) and $2R_g$ for chains with molecular mass of 670 K (sample f). The solid lines correspond to best-fits to eqn (1). See Table 1 for χ^2 values for fits.

Fig. 4 Interfacial broadening, $\Delta\sigma$, plotted as a function of time (t), for samples (c and h) with thickness h_f of each layer is about 45 nm annealed at 85 °C: sample c (□): d-PS(115 000 g mol^{-1})/h-PS(114 200 g mol^{-1}); sample h (○): d-PS(33 000 g mol^{-1})/h-PS(32 660 g mol^{-1}). The solid lines correspond to best-fits to eqn (1). See Table 1 for χ^2 values for fits.

limited for a reliable fitting to our model and in these cases we do not report values of τ and α in Table 1. However, we report the asymptotic value of the interfacial width, $\Delta\sigma(t \rightarrow \infty) \equiv \xi_p$, under these circumstances.

The relatively rapid evolution of $\Delta\sigma$ on the timescale of 1 h, followed by essentially no evolution in $\Delta\sigma$, has also been observed in several former studies when annealing above it's bulk T_g.[1–10] As mentioned in the introduction, this phenomenon has been attributed before to chain entanglement. Since we observe this 'caging' phenomenon regardless of whether the chains are above or below the entanglement molecular mass, this interpretation seems doubtful. Moreover, the appreciable temperature dependence of ξ_p is hard to reconcile with the notion of confinement within a tube.

The conformations of chains near interfaces can be expected to be different from those in the bulk because of distortion of chain conformation to minimize the interfacial energy and non-equilibrium conformations that arise during the film casting process.[40,41] We next consider some basic film properties that might reasonably be expected to reflect these changes in molecular conformation at interfaces. From Fig. 3, we observe that there is essentially no difference in the time dependence of $\Delta\sigma$ for the entangled polymers having molecular masses of
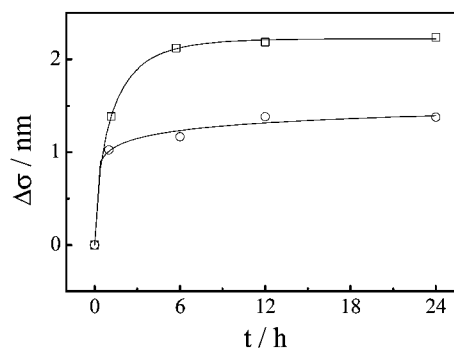
110 K and 670 K (well above $M_c \approx 38$ K). For samples d and e, the thickness of each layer is about 20 nm, which is about $2R_g$ for chains having a molecular mass of 110 K (sample d) and about $1R_g$ for chains with molecular mass of 670 K (sample e). For h_f smaller than the unperturbed chain size ($\approx 2R_g$), the chains should adopt a flatter conformation on average in comparison to bulk polymers. However, changing the film thickness in relation to the overall chain size (R_g) does not seem to influence the interfacial broadening kinetics in any significant so we do not see how a chain distortion effect can explain our observations. The same conclusion could also be drawn from thicker samples (c, f) where each layer has a thickness ≈ 45 nm. These thicknesses correspond to $\approx 5R_g$ for chains having a molecular mass ≈ 110 K (sample c) and to $\approx 2R_g$ for chains having a molecular mass of 670 K (sample f). Fig. 3 indicates that the thin film exhibits a different interfacial evolution than the thick films; ξ_p is smaller for thin film compared to the thick one. This change might be attributed to the interaction of the chains with the solid substrate, which is plausible given that Lin *et al.*[28,29] have showed that the substrate can affect polymer mobility for distances up to about 40 nm from the surface. Kuhlmann *et al.*[8] also found that attractive interactions between the chains and the substrate could slow the initial dynamics of thin film deposited directly on the substrate. We see thus that ξ_p varies from few nanometres (nm) near T_g to value near 1 nm at much lower temperatures. Table 1 also provides evidence that ξ_p decreases as the bilayer is made thinner or as the chain molecular mass decreases.

Table 1 Characteristics of the samples and parameters (ξ_p, τ, α) from fits to eqn (1)

Sample	d-PS/h-PS Molecular mass/g mol^{-1}	Thickness h_f/nm	Annealed temperature T/°C	$\Delta\sigma = \xi_p\{1 - \exp[-(t/\tau)^\alpha]\}$ ξ_p/nm	τ/h	α	χ^2
a	115 000/114 200	46.9/44.4	95	3.31	1.01	0.72	0.0004
b	115 000/114 200	50.2/47.8	90	2.86	1.45	0.61	0.08
c	115 000/114 200	50.7/47.4	85	2.22	1.20	0.71	0.04
d	115 000/114 200	20.0/23.1	85	1.28	1.88	0.35	0.34
e	673 600/641 340	19.0/24.0	85	1.42	1.93	0.31	0.49
f	673 600/641 340	50.3/42.7	85	2.30	1.07	0.69	0.01
g	673 600/641 340	46.1/39.9	95	3.41	0.94	0.72	0.002
h	33 000/32 660	45.7/41.6	85	1.72	1.83	0.20	0.31

Preparing unentangled lower molecular mass PS films (the 33 K sample) by the same floating method is a little bit tricky, since these films are characteristically more brittle and easier to fragment during preparation. The key is to keep water surface as still as possible during floating and collecting process. Note that a glass transition temperature change with molecular mass is not obvious in the range of our study. Therefore, the same annealing temperature for samples with different molecular masses should not be a problem. The motivation for using entangled polymer films for practical applications is then evident. Nonetheless, it is important to know whether the scale derives from chain entanglement and we thus prepared some unentangled bilayer films. Specifically, we compare sample c and sample h in Fig. 4, where h_f of each layer is about 45 nm and where both the samples were annealed at 85 °C. The polymers in sample h are unentangled and their molecular mobility should then be much higher than those of the other samples. We see that the plateau value of $\Delta\sigma$ for this unentangled sample (85 °C annealing) is lower than the other polymers samples having nearly the same h_f, but the plateau scale nonetheless exists. Entanglement is evidently not required to observe ξ_p, which provides a basic clue into the nature of this parameter.

Residual solvent effects are always a worry in the formation of polymer films, and we next consider how this might affect our observations. If there is residual solvent inside the films, it would evidently enhance the rate of interfacial relaxation at low temperatures and this effect could be especially large at the film boundaries if the solvent selectively segregates to the polymer interfacial region. To address this basic issue, a systematic study of residual solvent in PS films spin cast from toluene was recently performed. These measurements indicate that no detectable solvent exists in the as-cast PS films so we do not expect residual solvent to complicate our measurements.[42]

Now that the intrinsic nature of this interfacial healing length ξ_p has been established, we make some comments on the physical interpretation of this parameter. The relative insensitivity of this scale to M suggests that it might be related to the physics of glass-formation rather than entanglement. Superficially, we note that numerous recent measurements and simulation studies have indicated that glass-forming liquids are characterized by dynamic heterogeneities on the scale of 1 nm to 3 nm in the glass state.[43–45] Recent molecular dynamics simulations indicate that this heterogeneity in the glass state takes the form of an interpenetrating network structure in which regions of relatively high local stiffness interpenetrate relatively 'soft' regions in which molecular mobility is appreciably higher.[46,47] The simulations also indicate that the range of the elastic constant fluctuations can be modulated by varying the film thickness, the addition of molecular additives, etc. The basic picture obtained from the simulations is that a polymeric glass exhibits a structure (defined by elastic constant fluctuations rather than density fluctuations) that has the form of hierarchal 'sponge' structure; Zondervan et al. have recently advocated such a structure for glass-forming liquids based on macroscopic rheological and single particle orientational relaxation measurement.[48,49] Based on these simulation and experimental observations, we tentatively identify ξ_p as an interfacial healing length between the two polymeric glassy layers. It would be interesting to address this possibility directly in molecular dynamics simulations.

Another basic phenomenon is that the relaxation time for the interfacial relaxation is remarkably insensitive to molecular mass and the data in Table 1 even seem to suggest that the interfacial relaxation of the bilayer films annealed at 85 °C is even faster for the entangled polymer film, an effect exactly opposite from the relaxation being caused by large scale polymer chain diffusion. A very similar effect has recently been observed in the relaxation of surface relief patterns in 'nanoimprinted' unentangled and entangled PS films, where the imprinted patterns annealed at T_g were found to relax faster in the case of the entangled (1000 K molecular mass) polymer film than its unentangled (24 K molecular mass) counterpart.[50] A subsequent study by Ding et al. attributed this odd faster relaxation to the presence of residual stresses in entangled polymer films.[51]

It is certainly interesting that we see a similar relaxation trend with molecular mass trend in a polymer film never subjected to mechanical imprinting. The main effect that we observe, and noted also by Ding et al.,[51] is that the segmental rather than the chain relaxation dominates the interfacial relaxation, and the temperature dependence of this type of relaxation should be very similar for the 30 K and entangled polymer samples.[51] Again, the physics of glass-formation is implicated in the interfacial relaxation process.

Conclusions

Neutron reflectometry was used to study the initial 'burst regime' of interfacial relaxation[14,15] between polymer interfaces. The interfacial widths between deuterated polystyrene layer and normal polystyrene layer were systematically investigated as a function of time, sample thickness, molecular mass and for a range of annealing temperatures below the bulk glass transition temperature (85 °C to 95 °C). We found that the interface between the polymers broadens rapidly initially and the average interfacial width $\Delta\sigma(t)$ reaches a plateau value ξ_p that depends on the annealing temperature, T. This characteristic scale of interfacial broadening does not exhibit a dependence on molecular mass in entangled films and it is too small in comparison with independent estimates of the tube diameter. More basically, we observe the interfacial scale ξ_p regardless of whether the chains are entangled or not and the appreciable temperature dependence of ξ_p also makes this interpretation doubtful.

There have been other recent measurements demonstrating the existence of n interfacial layer of nanoscale thickness in glass-forming liquids.[52] Bell et al.[52] performed ion mobility measurements on amorphous 3-methyl pentane films in the glass state and observed a relatively high mobility in a skin layer at the vacuum–glass interface having a scale of about 3 nm and interfacial scale on the order of a few nanometres was observed by neutron reflectivity in glassy bilayers of hydrogenated and deuterated TNB [1,3-bis-(1-napthyl)-5-(2-napthyl) benzene]. Fakhraai and Forrest[53] have made some revealing measurements of the temperature dependence of relaxation in the near-surface region of glass films by adsorbing gold nanoparticles onto polymer films in the glass state, annealing the film above T_g so that particles sink into the film, followed by dissolving the gold with liquid mercury to create nanoholes in the polymer film. Further annealing of these hole patterns below the glass transition temperature indicated that these 'pot holes' created by the

deposited gold particles gradually fill in and the rate of this filling process was followed by atomic force microscopy (AFM). Apart from providing an unambiguous demonstration of a relatively high mobility in the interfacial layer of these polymer film (having a scale of roughly a few nm), this work indicates that the relaxation time governing this hole filling process has a weak temperature dependence in comparison with the bulk segmental relaxation time. The finding of a weak temperature dependence of the interfacial relaxation time is in broad accord with our observations (see Table 1). Our neutron reflectivity measurements provide the additional insight that the interfacial scale (ξ_p) of the enhanced interfacial mobility decreases upon cooling, an effect suggested before by Keddie et al.[54,55] We do not find a singular increase of ξ_p upon approaching T_g predicted by Keddie et al. Instead, ξ_p in our measurements varied over a modest range from 1 nm to 3 nm from temperatures well below T_g to about 5 °C below T_g, estimates that accord remarkably well with the scale (1–5 nm) of nanoparticles settling into PS films identified by Forrest and coworkers for a comparable temperature range.[56] On the other hand, Herminghaus and coworkers[57] estimated the thickness of a molten interfacial layer in emulsified PS droplets using NMR and interpreted their data as implying a 'surface melting' or a mobile interfacial layer whose thickness diverges in upon approaching T_g. This singular variation of the interfacial layer thickness seems rather out of line with our measurements, although both measurements point broadly to the existence of a mobile interfacial layer whose scale depends on temperature. Shifts of T_g with film thickness,[58] when the films are less than a 100 nm or so in thickness, is a complication in identifying quantitative trends of ξ_p with temperature and film thickness because this shift couples these variables strongly. A more quantitative study of ξ_p as function of film thickness and temperature will require a separate neutron reflectivity study that focuses on the effect of these variables over an extended range of these variables.

In the Introduction, we mentioned that measurements above T_g have indicated the existence of transient plateau scale ξ_p in the interfacial width $\Delta\sigma$, which naturally raises some questions about the interpretation of ξ_p in terms of the physics of glass formation. This can be readily explained by the emergence of transient dynamic heterogeneity well above the glass transition that is apparent in many simulation and experimental studies. For many amorphous glass-forming liquids, it has been noted that this heterogeneity first becomes prevalent experimentally (e.g., breakdown of Stokes–Einstein relation, splitting of α and β relaxation times in dielectric and structural relaxation),[59,60] below a characteristic 'crossover temperature' T_c that is often about 1.2 T_g. Previous work[61] has shown a change in the stability of thin PS films for temperatures near 1.2 T_g over a wide range of polymer molecular masses where T_g varied appreciably. Based on these considerations, we expect the scale to be emergent at temperatures below T_c rather than T_g. This hypothesis remains to be checked, however. At any rate, it is important to realize that the glass transition is very broad thermodynamic transitional phenomenon in terms of the temperature range involved and the onset of appreciable dynamic heterogeneity in glass-forming initiates well above T_g so that it makes good sense that ξ_p should be observed in interdiffusion measurements in the supercooled liquid, albeit transiently, for temperatures above T_g.

The existence of a nanoscale interfacial layer of relatively high molecular mobility in glassy polymer films has obvious implications for the frictional and adhesive properties of these films. An interfacial layer of this kind must also be relevant to understanding the stability of nanoimprinted patterns on thin polymer films, a topic of great interest for developing nanotechnology applications. There is evidence that the addition of antiplasticizer additives, which stiffen the polymer material in the glass state, can make polymer films much more abrasion resistant.[62] Recent simulations investigating the nature of antiplasticizer additives to polymer films show the existence of a nanoscale layer of enhanced collective molecular motion in pure polymer films[63–65] and that collective motion becomes highly attenuated by the antiplastizer additive. In particular, Riggleman et al.[63,64] find that the high surface mobility, corresponding of chain segments moving collectively, is largely attenuated in antiplasticized films. It would be interesting to investigate what effects such additives have on the surface inter-diffusion length ξ_p in measurements of the kind considered in the present paper.

We also plan to explore how ξ_p depends on monomer molecular structure and how this scale relates to the crossover scale at which deviations from bulk glass behavior are observed. In particular, the statistical segment length, rather than R_g, may be the appropriate dimension for gauging the onset of finite size effects on polymer film properties because of its influence on local molecular packing. Molecular dynamics simulations of coarse-grained polymer chains suggest an onset scale for finite size effects of roughly 20 to 30 bead diameters[66] where each bead models a statistical segment and the scale of statistical segment of a typical polymer chain can be taken to be on the order of 1 nm in dimensions. This gives an onset scale for finite size effects on thin polymer films of the right order of magnitude.

Acknowledgements

References and notes

1 A. Karim, A. Mansour, G. P. Felcher and T. P. Russell, *Phys. Rev. B: Condens. Matter*, 1990, **42**, 6846.
2 A. Karim, G. P. Felcher and T. P. Russell, *Macromolecules*, 1994, **27**, 6973.
3 T. P. Russell, V. R. Deline, W. D. Dozier, G. P. Felcher, G. Agrawal, R. P. Wool and J. W. Mays, *Nature*, 1993, **365**, 235.
4 G. Agrawal, R. P. Wool, W. D. Dozier, G. P. Felcher, T. P. Russell and J. W. Mays, *Macromolecules*, 1994, **27**, 4407.
5 G. Agrawal, R. P. Wool, W. D. Dozier, G. P. Felcher, J. Zhou, S. Pispas, J. W. Mays and T. P. Russell, *J. Polym. Sci., Part B: Polym. Phys.*, 1996, **34**, 2919.
6 M. Stamm, S. Hüttenbach, G. Reiter and T. Springer, *Europhys. Lett.*, 1991, **14**, 451.
7 K. Kunz and M. Stamm, *Macromolecules*, 1996, **29**, 2548.
8 T. Kuhlmann, J. Kraus, P. Müller-Buschbaum, D. W. Schubert and M. Stamm, *J. Non-Cryst. Solids*, 1998, **235**, 457.
9 G. Reiter and U. Steiner, *J. Phys. II*, 1991, **1**, 659.
10 M. Stamm and D. W. Schubert, *Annu. Rev. Mater. Sci.*, 1995, **25**, 325.
11 T. P. Russell, A. Karim, A. Mansour and G. P. Felcher, *Macromolecules*, 1988, **21**, 1890.
12 M. L. Fernandez, J. S. Higgins, J. Penfold, R. C. Ward, C. Shackleton and D. J. Walsh, *Polymer*, 1988, **29**, 1923.

13 M. Stamm, in *Physics of Polymer Surfaces and Interfaces*, ed. I. C. Sanchez, Butterworth-Heinemann Publishers, Boston, 1992, p. 163.
14 Y. H. Kim and R. P. Wool, *Macromolecules*, 1983, **16**, 1115.
15 H. Zhang and R. P. Wool, *Macromolecules*, 1989, **22**, 3018.
16 C. B. Gell, W. W. Graessley and L. J. Fetters, *J. Polym. Sci., Part B: Polym. Phys.*, 1997, **35**, 1933.
17 S. J. Whitlow and R. P. Wool, *Macromolecules*, 1989, **22**, 2648.
18 S. J. Whitlow and R. P. Wool, *Macromolecules*, 1991, **24**, 5926.
19 P.-G. de Gennes, *J. Chem. Phys.*, 1971, **55**, 572.
20 P.-G. de Gennes, *Scaling Concepts in Polymer Physics*, Cornell University Press, Ithaca, NY, 1979.
21 M. Doi and S. F. Edwards, *The Theory of Polymer Dynamics*, Oxford University Press, Oxford, 1986.
22 K. Kremer, G. S. Grest and I. Carmesin, *Phys. Rev. Lett.*, 1988, **61**, 566.
23 D. Richter, B. Farago, L. J. Fetters, J. S. Huang, B. Ewen and C. Lartigue, *Phys. Rev. Lett.*, 1990, **64**, 1389.
24 M. Stamm, *Adv. Polym. Sci.*, 1992, **100**, 357.
25 S. Prager and M. Tirrell, *J. Chem. Phys.*, 1981, **75**, 5194.
26 S. Prager, D. Adolf and M. Tirrell, *J. Chem. Phys.*, 1983, **78**, 7015.
27 P.-G. de Gennes, in *Physics of Polymer Surfaces and Interfaces*, ed. I. C. Sanchez, Butterworth-HeinemannPublishers, Boston, 1992, p. 55.
28 E. K. Lin, W. L. Wu and S. K. Satija, *Macromolecules*, 1997, **30**, 7224.
29 E. K. Lin, R. Kolb, S. K. Satija and W. L. Wu, *Macromolecules*, 1999, **32**, 3753.
30 J. D. Ferry, *Viscoelastic Properties of Polymers*, Wiley, New York, 3rd edn, 1980.
31 Certain commercial materials and instruments are identified in this article to adequately specify the experimental procedure. In no case does such identification imply recommendation or endorsement by the National Institute of Standards and Technology, nor does it imply that materials or equipment identified are necessarily the best available for the purposes.
32 N. Awaji, Y. Sugita, S. Ohkubo, T. Nakanishi, K. Takasaki and S. Komiya, *Jpn. J. Appl. Phys.*, 1995, **34**, 1013.
33 Y. Sugita, S. Watanabe and N. Awaji, *Jpn. J. Appl. Phys.*, 1996, **35**, 5437.
34 J. F. Ankner, C. F. Majkrzak and S. K. Satija, *J. Res. Natl. Inst. Stand. Technol.*, 1993, **98**, 47.
35 J. A. Dura, D. J. Pierce, C. F. Majkrzak, N. Maliszewskyj, D. J. McGillivray, M. Lösche, K. V. O'Donovan, M. Michailescu, U. A. Perez-Salas, D. L. Worcester and S. H. White, *Rev. Sci. Instrum.*, 2006, **77**, 074301.
36 P. A. Kienzle, K. V. O'Donovan, J. F. Ankner, N. F. Berk and C. F. Majkrzak, http://www.ncnr.nist.gov/reflpak, 2000–2006.
37 J. F. Douglas, H. E. Johnson and S. Granick, *Science*, 1993, **262**, 2010.
38 A. Karim, V. V. Tsukruk, J. F. Douglas, S. K. Satija, L. J. Fetters, D. H. Reneker and M. D. Foster, *J. Phys. II*, 1995, **5**, 1441.

39 C. A. Angell, *Science*, 1995, **267**, 1924.
40 S. K. Kumar, M. Vacatello and D. Y. Yoon, *J. Chem. Phys.*, 1988, **89**, 5206.
41 W. G. Madden, *J. Chem. Phys.*, 1987, **87**, 1405.
42 X. Zhang, K. G. Yager, S. Kang, N. J. Fredin, B. Akgun, S. Satija, J. F. Douglas, A. Karim and R. L. Jones, *Macromolecules*, 2010, **43**, 1117.
43 E. Hempel, G. Hempel, A. Hensel, C. Schick and E. Donth, *J. Phys. Chem. B*, 2000, **104**, 2460.
44 X. H. Qiu and M. D. Ediger, *J. Phys. Chem. B*, 2003, **107**, 459.
45 K. S. Schweizer and E. J. Saltzman, *J. Chem. Phys.*, 2004, **121**, 1984.
46 K. Yoshimoto, T. Jain, K. V. Workum, P. F. Nealey and J. J. De Pablo, *Phys. Rev. Lett.*, 2004, **93**, 175501.
47 R. A. Riggleman, J. F. Douglas and J. J. de Pablo, *Soft Matter*, 2010, **6**, 292.
48 R. Zonderman, F. Kulzer, G. C. G. Berkhout and M. Orrit, *Proc. Natl. Acad. Sci. U. S. A.*, 2008, **104**, 12628.
49 R. Zondervan, T. Xia, H. van der Meer, C. Storm, F. Kulzer, W. van Saarloos and M. Orrit, *Proc. Natl. Acad. Sci. U. S. A.*, 2008, **105**, 4993.
50 Y. Ding, H. W. Ro, J. F. Douglas, R. L. Jones, D. R. Hine, A. Karim and C. L. Soles, *Adv. Mater.*, 2007, **19**, 1377.
51 Y. Ding, H. W. Ro, T. A. Germer, J. F. Douglas, B. C. Okerberg, A. Karim and C. L. Soles, *ACS Nano*, 2007, **1**, 84.
52 R. C. Bell, H. Wang, M. J. Iedema and J. P. Cowin, *J. Am. Chem. Soc.*, 2003, **125**, 5176.
53 Z. Fakhraai and J. A. Forrest, *Science*, 2008, **319**, 600.
54 J. L. Keddie, R. A. L. Jones and R. A. Cory, *Faraday Discuss.*, 1994, **98**, 219.
55 J. L. Keddie, R. A. L. Jones and R. A. Cory, *Europhys. Lett.*, 1994, **27**, 59.
56 M. Ilton, D. Qi and J. A. Forrest, *Macromolecules*, 2009, **42**, 6851.
57 S. Herminghaus, R. Seemann and K. Landfester, *Phys. Rev. Lett.*, 2004, **93**, 017801.
58 P. A. O'Connell and G. B. McKenna, *J. Polym. Sci., Part B: Polym. Phys.*, 2009, **47**, 2441.
59 M. Beiner, H. Huth and K. Schroter, *J. Non-Cryst. Solids*, 2001, **279**, 126.
60 R. Richert, *J. Phys.: Condens. Matter*, 2002, **14**, R-703.
61 K. M. Ashley, D. Raghavan, J. F. Douglas and A. Karim, *Langmuir*, 2005, **21**, 9518.
62 P. E. Cais, M. Nozomi, M. Kawai and A. Miyake, *Macromolecules*, 1992, **25**, 4588.
63 R. A. Riggleman, K. Yoshimoto, J. F. Douglas and J. J. de Pablo, *Phys. Rev. Lett.*, 2006, **97**, 045502.
64 R. A. Riggleman, J. F. Douglas and J. J. de Pablo, *J. Chem. Phys.*, 2007, **126**, 234903.
65 R. A. Riggleman, J. F. Douglas and J. J. de Pablo, *Phys. Rev. E: Stat. Phys., Plasmas, Fluids, Relat. Interdisc. Top.*, 2007, **76**, 011504.
66 K. Kim and R. Yamamoto, *Phys. Rev. E: Stat. Phys., Plasmas, Fluids, Relat. Interdisc. Top.*, 2000, **61**, 41.